History and Physical Significance of the Roughness Froude Number

TONY L. WAHL, P.E. (IAHR Member), Technical Specialist, *Hydraulics Laboratory, Bureau of Reclamation, Denver, Colorado, USA*

Email: twahl@usbr.gov

History of the Roughness Froude Number

History and Physical Significance of the Roughness Froude Number

ABSTRACT

The roughness Froude number is a relatively new dimensionless parameter that began appearing in the hydraulic engineering literature in the late 1970s, first for the analysis of aeration inception in smooth chutes, and then later in connection with stepped chutes. This article reviews its foundations, historical development, alternative forms, present-day applications, and physical significance, which has received little attention previously. In addition to its empirically demonstrated connection to aeration inception, this paper shows that one form of a roughness Froude number has a strong relation to the transition between nappe and skimming flow regimes of stepped chutes, while another combines the dimensionless flow friction factor and the relative submergence of roughness elements.

Keywords: Aerated flow; aeration inception; boundary layer; nappe flow; roughness Froude number; skimming flow; stepped chutes.

1 Introduction

Several dimensionless groupings of variables described as roughness Froude numbers are used today to analyze aeration associated with steady-state flows in both smooth and stepped chutes (e.g., Chanson 1994a, 1994b, 2002; Boes & Hager 2003a, 2003b; Hunt et al. 2014). They arose from several related parameter groups that appeared in the hydraulic engineering literature in the late 1970s and early 1980s (Keller & Rastogi 1977; Cain & Wood 1981; Wood et al. 1983). The roughness Froude number has been related to the inception point of aerated flow, and its predecessor, the inception Froude number, is based on the depth and velocity of flow at the inception point, quantities that serve as reference values for defining the aerated flow conditions in the downstream developing aerated flow zone. The most common form, which appeared first in Cain and Wood (1981), is:

$$F_* = \frac{q}{\sqrt{g \sin(\theta) k_s^3}} \tag{1}$$

where F_* is the roughness Froude number, q is discharge per unit width, g is acceleration due to gravity, $\sin(\theta)$ is slope, θ is chute slope angle, and k_s is a reference length serving as a measure of surface roughness (e.g., sand grain roughness, or a roughness dimension related to step height).

The location of air entrainment inception for both smooth and stepped chutes has been empirically related to F_* for a wide range of slope and roughness conditions (e.g., Cain & Wood 1981; Chanson 1994b; Boes & Hager 2003a; Hunt & Kadavy 2013). The initiation of air entrainment is widely recognized to involve inertia, gravitational forces, surface

tension, turbulence, and characteristics of the boundary layers developed along the chute floor and in the water and air layers adjacent to the air-water interface (e.g., Valero & Bung 2016). The F_* parameter incorporates many of these factors, although surface tension is notably lacking and nothing in the parameter relates to the air layer above the water surface. These factors may have limited variation or significance for prototype scale flows or appropriately sized laboratory studies (Pfister & Chanson 2014), allowing F_* to adequately represent the dimensionless combination of the practically important variables for steep chutes, where turbulence intensity is almost always high enough to initiate self-aeration once the turbulent boundary layer begins to interact with the free surface.

Several variations of the roughness Froude number have been used to characterize the flow in stepped chutes (Fig. 1), with the reference length being either the depth of the step cavity perpendicular to the pseudobottom (the line connecting the step tips), $k_s = h \cdot \cos(\theta)$, or the vertical step height, h. Regardless of the details, when described as roughness Froude numbers the dimensionless groupings have typically included the unit discharge, gravity and slope terms, and a reference length term related to the size of the roughness elements affecting the flow. Terrier (2016) noted variations using either $h \cdot \cos(\theta)$ or h as reference lengths and $\sin(\theta)$ or $\tan(\theta)$ slope terms in the denominator.

Since these dimensionless quantities are described as Froude numbers, it is useful to recall the traditional definition for the Froude number of an open-channel flow in a rectangular channel:

$$F = \frac{V}{\sqrt{gD}} = \frac{q/D}{\sqrt{gD}} = \frac{q}{\sqrt{gD^3}} \tag{2}$$

where V is the flow velocity and D is the flow depth. This Froude number represents the ratio of inertial and gravitational forces (strictly speaking, the square root of that ratio). For steep slopes, Chow (1959) provided a modified form:

$$F = \frac{V}{\sqrt{gD \cdot \cos\theta}} = \frac{q}{\sqrt{gD^3 \cdot \cos\theta}} \tag{3}$$

with $D \cdot \cos(\theta)$ representing the piezometric head associated with depth D measured normal to the channel boundary. Comparing Eqs. (1) and (3), the general form and dimensional similarity of the flow and roughness Froude numbers is evident. Differences between them are the use of a reference length related to the roughness element size instead of the flow depth and the use of $\sin(\theta)$ rather than $\cos(\theta)$.

2 Emergence and evolution of the roughness Froude number

2.1 The boundary layer and aerated flow in smooth chutes

The streamwise development of aerated flow in spillways and other smooth- and rough-bottom chutes is a dramatic visual phenomenon that has long held the interest of hydraulic engineers, with profound effects on flow energy, depth, frictional resistance, and water quality (Fig. 2). Lane (1939) was first to make a suggestion that the inception of aerated flow and the appearance of whitewater in steep spillway chutes occurs when the boundary layer created by friction at the bed grows in thickness to the point where it intersects the free water surface. Boundary layer growth and its relation to the inception point was subsequently studied by several researchers, including Bauer (1954), Halbronn (1954), Campbell et al. (1965), Cassidy (1966), Bauer (1966), and Gangadharaiah et al. (1970). Other mechanisms may also be at work in some cases, such as growth of longitudinal vortices (Levi 1967) and interaction between the flowing water at the surface and the air flow induced above the water surface (Valero & Bung 2016). Valero and Bung (2016) summarize experimental evidence suggesting that the inception point commonly occurs before the computed intersection of the boundary layer and the water surface, i.., when the ratio of the boundary layer thickness to the flow depth is about 0.8.

Straub and Anderson (1958) and Killen (1968) performed foundational laboratory studies of aerated flow, describing the inception of visible aeration at the surface and measuring depth-wise profiles of air concentration along the length of chutes as air bubbles migrated from the surface toward the bottom in the developing flow downstream from the inception point. Researchers have identified zones of blackwater or clearwater flow (no aeration), developing partially aerated flow (air entrained near the water surface, but no air yet reaching the bed), developing fully aerated flow (measurable air present within the flow from surface to bed), and fully developed aerated flow (time-averaged equilibrium velocity and air entrainment conditions not changing with increasing distance down the chute). Defining the aeration inception point has long been of interest to spillway designers, and the flow conditions at the inception point (velocity and depth) have served as key reference quantities for modeling the subsequent developing zones of aerated flow. Although laboratory investigations have provided the bulk of our understanding of aerated flow in chutes, scale effects in two-phase air-water flows (Pfister & Chanson 2014) have made observations and measurements of aerated flow in full-size spillways especially valuable. Important efforts in this area include those of Keller (1972), Cain and Wood (1981) and more recently Hohermuth et al. (2021). These early field studies would underpin the emergence of the roughness Froude number

Professor Ian Wood and several postgraduate students at the University of Canterbury made significant early studies of prototype-scale aerated flows. The Ph.D. thesis of Robert Keller (1972) investigated aeration inception in detail and reported field measurements of self-aerated flow from the 45° sloped face of the spillway of New Zealand's Aviemore Dam. The measurements were concentrated in the developing region between the inception point and the fully developed aerated zone. Using dimensional analysis, Keller (1972) developed a parameter that he described as an "inception Froude number":

$$\frac{V_i}{\sqrt{gSD_i}} \tag{4}$$

in which V_i and D_i are the flow velocity and depth at the point of aeration inception, and $S = \sin(\theta)$ is the channel slope. With the channel slope term, $S = \sin(\theta)$, in the denominator, Eq. (4) no longer represents the same ratio of inertial and gravitational forces as Eqs. (2) or (3). However, the dimensionless ratio in Eq. (4) can be viewed as the square root of the ratio of inertial forces to friction forces at the bed (gSD representing shear at the boundary), which is the inverse square root of the flow friction factor. Such an interpretation was not suggested by Keller (1972).

The slope definition used in Eq. (4) is the same as that used in Bauer's (1954) boundary layer studies. It should be noted that this makes the slope equal to the change in elevation per unit of distance *along the slope*, which is the common usage in steep chutes and differs from the traditional mathematical definition of slope in Cartesian coordinates as vertical change per unit of horizontal run. With the latter definition, true mathematical slope would be $\tan(\theta)$ rather than $\sin(\theta)$. The difference is significant for slopes steeper than about 5° and more significant with increasing θ.

Keller (1972) used the data from the MEng thesis of Lai (1971) to determine values of the inception Froude number for model chutes over a range of slopes. Keller, Lai and Wood (1974) prepared an article combining these works, and the appendix to that paper presented a basic physical argument for the development of the inception Froude number, illustrating how S arrived in the denominator. The Ph.D. thesis of Cain (1978), another student of Wood, also used this inception Froude number.

The inception Froude number as defined above is similar to the traditional flow Froude number, Eq. (2), except for the inclusion of the channel slope term in the denominator. Keller's thesis (1972) and the appendix of Keller, Lai and Wood (1974) show that the slope term arises from an estimate of the velocity at the inception point being

$$V_I \approx \sqrt{2gS \cdot x_i} \tag{5}$$

with x_i being the distance along the slope from the start of the chute and the $S{\cdot}x_i$ term being the vertical elevation drop over that distance, which represents the approximate energy head

at the inception point, assuming minimal losses. Note that if the vertical elevation drop had been specified directly, not as a function of x_i, then $S = \sin(\theta)$ would have been absent from Eq. (5) and from what follows. Rearranging Eq. (5) to isolate x_i produces

$$x_i = \frac{V_i^2}{2gS} \tag{6}$$

Noting that the Darcy friction factor in a wide, open channel is $f = 8gDS/(V)^2$, the distance x_i given by Eq. (6) is proportional to the ratio of the flow depth and the friction factor. Eq. (6) can be combined with empirical equations for estimating the boundary layer thickness at the inception point (where the flow depth is designated D_i). For a rough-bed case the boundary layer thickness δ is a function of the flow distance x_i and the equivalent sand-grain roughness dimension ϵ (Keller, Lai & Wood 1974; Halbronn 1952, 1954), i.e.:

$$D_I = \delta = 0.0447\epsilon^{0.154} x_i^{0.846} = 0.0447\epsilon^{0.154} \left(\frac{V_i^2}{2gS}\right)^{0.846} \tag{7}$$

After rearranging, S appears in the denominator of a dimensionless ratio that includes V_i and D_i :

$$\frac{V_i}{\sqrt{gSD_i}} = 8.88 \left(\frac{D_i}{\epsilon}\right)^{0.091} \tag{8}$$

The quantity on the left side of Eq. (8) is the inception Froude number, Eq. (4). For a smooth-bed case, a similar development produces (Keller, Lai & Wood 1974):

$$\frac{V_I}{\sqrt{gSD_i}} = 20.65(S^{0.0285} D_i^{0.087}) \tag{9}$$

Keller (1972) showed that this modified Froude number in the left side of Eqs. (8) and (9) has a nearly constant value of about 15.8 to 16.4 at the point of aeration inception over a range of flow rates and at different slopes and roughnesses when considering both his own data and those of Lai (1971). This is consistent with the small values of the exponents in the right-hand terms of Eqs. (8) and (9). However, it would have been equally valid to keep $S = \sin(\theta)$ out of the dimensionless ratio (since it contributes no dimensions) and conclude (in both rough- and smooth-bed cases since the exponent of S in the right-hand side of the smooth-bed equation is nearly zero) that

$$\frac{V_i}{\sqrt{gD_i}} \propto \sqrt{S} = \sqrt{\sin\theta} \tag{10}$$

or

$$\frac{V_i}{\sqrt{gD_i \cos(\theta)}} = \frac{q}{\sqrt{gD_i^3 \cos(\theta)}} \propto \sqrt{\frac{\sin\theta}{\cos\theta}} = \sqrt{\tan\theta} \tag{11}$$

In the last form, the slope-adjusted Froude number familiar to most hydraulicians is proportional to the square root of the mathematical slope. It should be emphasized that the inception Froude number—like the traditional flow Froude number—contains velocity and reference lengths related only to the water flow.

A switch from the flow-related length reference D_i in Eq. (11) began with work by Keller and Rastogi (1975) that showed agreement between aeration inception and theoretical predictions of the intersection of the boundary layer and the water surface, using experimental data from a laboratory channel, a full-size overflow spillway, and a full-size gated spillway. Subsequently, Keller and Rastogi (1977) provided design curves for predicting the inception point and related the inception point through dimensional analysis to the channel slope and the dimensionless combination $q/(gk_s^3)^{1/2}$. They did not assign a symbol or a name to this dimensionless group, which notably did not include a slope-related term or a reference length related to the flow depth.

The next important step in the development of the roughness Froude number was due to Cain and Wood (1981). Again reporting prototype data from Aviemore spillway, they applied the symbol F_* to a dimensionless parameter described as a "Froude number based on design quantities":

$$F_* = \frac{q}{\sqrt{gSk_s^3}} \tag{12}$$

where S is the slope, $\sin(\theta)$. This dimensionless parameter was similar to the parameter suggested by Keller and Rastogi (1977), but added the $\sin(\theta)$ term of the inception Froude number. Unlike the inception Froude number, F_* did not represent solely the properties of the flow, but instead a combination of flow (q) and chute roughness (k_s) properties. Cain and Wood (1981) presented relations for predicting the inception point, inception depth, and inception velocity as a function of this new Froude number. Cain and Wood (1981) did not explain what inspired them to use a hybrid parameter, and no derivation justifying the placement of S in the denominator was given. The author speculates that S was included for consistency with the form of the inception Froude number developed by Keller, Lai and Wood (1974), while the roughness-based length reference apparently followed Keller and Rastogi (1977), although Cain and Wood (1981) only cited Keller and Rastogi (1975). The $g{\cdot}S$ variable combination was explained to physically represent the component of gravity acting parallel to the spillway slope. This is in contrast to $g{\cdot}\cos(\theta)$ in the traditional slope-adjusted Froude number of Chow (1959), which represents the component of gravity acting perpendicular to the slope and drives the depthwise distribution of pressure within the flow. The gravity component parallel to the slope is the force that accelerates and maintains the flow, but it is not apparent why this should appear in relations applying to air inception when

the normal gravitational component is key for the flow of water. No investigator has offered a derivation of Eq. (12) based on first principles. However, rearrangement reveals an alternate physical interpretation as a quantity proportional to the ratio of the 1.5 power of the relative submergence of roughness elements and the square root of the friction factor:

$$F_* = \frac{q}{\sqrt{gSk_s^3}} = \frac{VD}{\sqrt{gSk_s^3}}\frac{\sqrt{D}}{\sqrt{D}} = \frac{V}{\sqrt{gDS}}\left(\frac{D}{k_s}\right)^{3/2} = \sqrt{\frac{8}{f}}\left(\frac{D}{k_s}\right)^{3/2} \quad (13)$$

Like Eq. (6), this suggests the strong connection between frictional resistance and boundary layer growth leading to air entrainment.

Wood et al. (1983), citing the previous work by Cain and Wood (1981), used F_* again as defined in Eq. (12) to predict the inception point in smooth chutes, calling it simply a "discharge parameter". They also noted the similarity between F_* and the dimensionless combination $q/(gk_s^3)^{1/2}$ suggested by Keller and Rastogi (1977).

2.2 Stepped chutes and the naming of the roughness Froude number

Following the burst of research activity on the inception point for smooth spillways in the 1970s and early 1980s, the F_* parameter lay dormant for about a decade. The 1990s brought a period of strong research interest in stepped chutes constructed from conventional concrete, masonry, and a relatively new construction material growing rapidly in popularity, roller-compacted concrete (RCC). Chanson (1994a), another student of Wood, cited the relations from Wood et al. (1983) for predicting the location and flow properties of the aeration inception point in stepped channels, calling F_* simply "a Froude number". In the first of two books on stepped chutes, Chanson (1994b) cited both Keller and Rastogi (1977) and Wood et al. (1983) and described $F_* = q/[g \sin(\theta)k_s^3]^{1/2}$ as a "Froude number defined in terms of the roughness height". Subsequent works (e.g., Chanson 2002; Felder & Chanson 2009, 2011, 2013, 2016) have used similar descriptions while typically citing only Wood et al. (1983) or no specific source.

At an International Workshop on Hydraulics of Stepped Spillways held in Zurich, Switzerland, Boes and Minor (2000) and Hager and Boes (2000) described F_* as the "roughness Froude number", a condensation of Chanson's description. Both papers defined F_* using the vertical step height:

$$F_* = \frac{q}{\sqrt{g \sin(\theta)h^3}} \quad (14)$$

These papers included the slope term in the denominator, following the lead of Cain and Wood (1981) and Wood et al. (1983). Boes and Minor (2000) related F_* to the location of the inception point and to the bottom air concentration at locations downstream from inception.

Hager and Boes (2000) used F_* to predict the depth of the aerated flow mixture in the fully developed zone. Following these papers, Boes and Hager (2003a, 2003b) used F_* again as defined in Eq. (14) in a pair of articles on aerated flow and general hydraulic design of stepped spillways. These have been more readily available than the conference papers from the 2000 workshop and have thus been widely cited during the past two decades. Most subsequent works that apply a roughness Froude number to stepped spillways or smooth chutes have used the form of either Eq. (14) or Eq. (1) and cited either Boes and Hager (2003a; 2003b), Cain and Wood (1981), Wood et al. (1983) or Chanson (1994a, 1994b, 2002) as the source of the parameter. Cheng et al. (2014), studying boundary layers of stepped chutes, cited Keller and Rastogi (1977), but included the sin(θ) term in the denominator as used in the other references listed above. The most useful definition for F_* has been the form shown in Eq. (1), with the length reference set to the step cavity depth normal to the slope line, $k_s = h \cdot \cos(\theta)$. This form makes the parameter adaptable to modified step shapes, such as beveled faces common to RCC overlays used for embankment dam overtopping protection (Hunt et al. 2022).

A handful of recent works have used dimensionless parameters like the roughness Froude number, but without a slope term in the denominator [similar to Keller & Rastogi (1977)]. Mateos and Elviro (1997) presented data on the initiation of aeration in ten stepped spillway models for six Spanish dams with slopes in a narrow range from 51° to 53°. They did not use the roughness Froude number name, but proposed:

$$\frac{Z}{h} = 5.6 \left(\frac{q}{\sqrt{g h^3}} \right)^{0.8} \tag{15}$$

with Z being the vertical drop from the spillway crest to the inception point. Hiller et al. (2019) also omitted the slope term from a stone Froude number used to analyze riprap performance, $F_S = q/(g d^3)^{1/2}$, with d being the stone diameter. Many investigations have analyzed data pertaining to only a single slope (e.g., Meireles & Matos 2009; Amador et al. 2009) and have related the roughness Froude number with the included slope term to the inception distance along the slope and the inception flow depth; omitting the slope term would have yielded relationships of similar quality with adjusted coefficient values.

3 Physical significance of the roughness Froude number

The traditional Froude number uses reference quantities (velocity and flow depth) that are both related to bulk properties of the flowing water. In contrast, the roughness Froude number is a hybrid parameter, mixing reference quantities that relate to flow (unit discharge, q) and properties of the flow boundary (roughness length, k_s). Even expanding and separating terms, the quantity q/k_s does not represent a real velocity, but instead a fictitious velocity that

would result from passing all of the flow *through* the space occupied by the roughness elements. Additionally, the $(gk_s)^{1/2}$ term is not related to flow, whereas the $(gD)^{1/2}$ term in the flow Froude number represents shallow wave celerity or gravitational forces applied to the flowing water. It could be argued that $(gk_s)^{1/2}$ represents gravitational forces applied to the water contained in the spaces between the roughness elements (interstitial flow if the surface layer were composed of something porous like stone riprap). Other forms of Froude numbers used in specialized hydraulic engineering applications use mixed references to both flow quantities and channel bed or transported object characteristics. For example, the densimetric Froude number used to model floating vessels and debris uses the flow velocity and a characteristic length of the modeled object, with an adjustment to account for buoyancy (Ettema et al. 2000). The familiar Shields parameter used to model bed sediment movement can be viewed as the square of a densimetric Froude number involving the shear velocity of the flow and the bed particle length scale, again with a density factor. It can be interpreted physically as the ratio of the driving force (drag, or bed shear stress) to the resisting force (particle weight and friction). Finally, a particle densimetric Froude number using the mean flow velocity and the sediment particle size has been proposed by Aguirre-Pe et al. (2003) for sediment transport applications. These examples show that there can be utility in mixing reference quantities related to both the flow and boundaries or objects.

The traditional flow Froude number is associated with distinct flow regimes in open channel flow that have distinct mechanical characteristics. $F<1$ indicates subcritical flow in which waves are able to travel both upstream and downstream so that downstream conditions may affect the upstream flow, while $F>1$ indicates supercritical flow in which all waves are swept downstream and there is an absolute separation between downstream and upstream conditions. Froude numbers in other scientific fields also relate to fundamental changes in mechanical behavior. For example, in the field of gait analysis, a walking Froude number, $F_W = v^2/gL$, may be computed representing the ratio of centripetal force to the weight of the walking animal for an inverted pendulum that represents the walking limb (Vaughan & O'Malley 2005). The travel speed is v and the characteristic length, L, is often taken to be the total length of the leg or the height of the hip joint. ($F_W{}^{1/2}$ is dimensionally analogous to the flow Froude number, and is described by Vaughan and O'Malley as the dimensionless velocity, β.) In bipeds, $F_W = 1$ represents the theoretical limit for walking, as any larger value indicates that the foot will fail to strike the ground before the leg swing repeats; the practical transition from walking to running tends to occur before this limit is reached, at around $F_W = 0.5$ (Alexander 1989). Most medium to large quadrupeds switch from a traditional walk to a symmetric running gait (trot or pace) at about $F_W = 1$, and a transition to asymmetric gaits (e.g., canter, transverse gallop, rotary gallop, bound, or pronk) occurs around $F_W = 2$ or 3 (Alexander 1984). There is some variation of these gait transition values among small

animals that are not subject to the limitations on bone and muscle stress that occur at larger scales (Alexander and Jayes 1983; Biewener 1989; Alexander 2005), but general dynamic similarity is seen across many classes of ground-based animals.

Gait analysis related to other forms of locomotion could make use of the Froude number. In wing-propelled (flapping) flight, distinct gaits and wing stroke mechanics have been recognized at different flight speeds (Rayner et al. 1986). Gaits in the swimming of fish have also been observed, with shifts from propulsion by alternating pectoral fin motions (left-right) at low speeds to synchronous (in-phase) pectoral fin movements at moderate speed and finally to axial propulsion by movements of the whole body and tail (caudal fin) at high speeds (Hale et al. 2006; Gibb et al. 1994). Flying and swimming gaits have not been analyzed in a fully dimensionless way, although gait transitions in fish have been related to relative swimming speeds expressed in body lengths per unit time. A flying or swimming Froude number has not been applied to either the flight or swimming cases, but one could be formed using body length or wing characteristic dimensions that might correlate with flying and swimming gait changes in a manner analogous to the ground-based gait studies. These applications of various Froude numbers in a range of sciences exhibit the potential for such parameters to relate to fundamental shifts in mechanical behavior, but no similar explanation has been previously offered for the roughness Froude number.

The most apparent change in the mechanics of stepped chute flow is the transition between the nappe and skimming flow regimes (Fig. 3). Nappe flow occurs when each step functions independently as a free overfall, with subcritical flow on the tread, critical flow at the brink of each step, and a hydraulic jump on the tread of the next step. Transitional subregimes of nappe flow have been described, based on the flow condition on the tread as influenced by the next downstream step: either a fully developed hydraulic jump, partially developed jump, or no jump (Chanson 1994b). Skimming flow occurs when the flow is supercritical and nearly uniform from the tip of one step to the next, forming enclosed rotating vortices in the lee of each step (Figs 1 and 3). Streamlines illustrated from CFD studies by Cheng et al. (2014) demonstrate that even in skimming flow, each step tip significantly affects the flow. Data compiled by Chanson and Toombes (2004) and Kramer and Chanson (2018) indicate the approximate boundaries of the transitional ranges.

The transition from nappe to skimming flow has been related to the dimensionless combination d_c/h, with d_c being the critical depth, $(q^2/g)^{1/3}$ in a wide channel, and h the vertical step height (Chanson 2002; Boes & Hager 2003b; Ohtsu et al. 2001, 2004). More refined studies of the transition zone show that it spans a range of values of d_c/h, with a lower limit defining the boundary between nappe flow and transitional skimming flow and an upper limit defining the boundary between the transitional range and fully skimming flow. Chanson and Toombes (2004) suggested curves defining the relation between d_c/h and the chute slope

at both edges of the transitional range. These expressions can also be converted to the ratio d_c/k_s, with $k_s = h \cdot \cos(\theta)$.

The ratio $[d_c/(k_s \sin(\theta)^{0.5})]^{1.5}$ is equal to the roughness Froude number as defined in Eq. (1) $[d_c/(k_s \sin(\theta)^{0.5})]^{1.5} = q/(g \sin(\theta) k_s^3)^{1/2}$. If the $\sin(\theta)$ terms are replaced by $\cos(\theta)$ to incorporate the gravitational component that is normal rather than parallel to the chute slope, then $[d_c/(k_s \cos(\theta)^{0.5})]^{1.5} = q/(g \cos(\theta) k_s^3)^{1/2}$. Figures 4 and 5 show plotted values of these expressions for the transitional threshold curves of Chanson and Toombes (2004) and data points compiled by Kramer and Chanson (2018) at the nappe-transition and transition-skimming flow boundaries. For the expression using $\cos(\theta)$ in the denominator, the lower bound of the transitional range is insensitive to slope and is in the range of $q/(g \cos(\theta) k_s^3)^{1/2} \approx 0.5$ to 1.0. The expression using $\sin(\theta)$ in the denominator exhibits large variation with slope (Fig. 5). It is hypothesized here that a roughness Froude number defined as $F_* = q/(g \cos(\theta) k_s^3)^{1/2}$ provides a physically-based parameter that is related to the mechanical changes in flow structure that occur in the transition from nappe to skimming flow, and this explains the relatively constant transition range boundaries in Fig. 4.

4 Closing remarks

The development of the roughness Froude number has followed an indirect path, beginning with research on the aeration inception point of prototype smooth chutes by Prof. Ian Wood and his postgraduate students at the University of Canterbury. Although empirically shown to have great usefulness, the parameter has never been derived from basic fluid mechanics principles but arises primarily from dimensional considerations. Its roots lie in an inception Froude number based entirely on flow-related references (discharge and flow depth), but the roughness Froude number is a hybrid that adopts similar mathematical form while combining flow and boundary roughness references (discharge and step height or roughness size). The $\sin(\theta)$ term in the denominator of the most commonly used form seems to be an artifact of the choice made in the development of the inception Froude number to express the energy head of the flow at the inception point as a function of the distance traveled along the channel slope, rather than the explicit vertical drop. An alternate interpretation relying on the $\sin(\theta)$ term is that the roughness Froude number is proportional to the ratio of the 1.5 power of the relative submergence of roughness elements and the square root of the friction factor.

Use of the roughness Froude number in studies of aeration inception for both smooth and stepped chutes has become so widespread that many recent references give no citations to its origin, just as most hydraulic researchers do not cite the origins of such ubiquitous concepts as the Froude number, Reynolds number, and Chezy, Manning, and Darcy-Weisbach frictional resistance models. Keller and Rastogi (1977) were the first to present the

parameter in approximately the functional form now commonly used, but they did not include the sin(θ) term in the denominator and did not identify the variable grouping with a distinct name or symbol. Cain and Wood (1981) and Wood et al. (1983) added the sin(θ) term and suggested the F_* symbol. In the stepped chute arena, Chanson (1994b, 2002), Boes and Minor (2000), Hager and Boes (2000), and Boes and Hager (2003a, 2003b) applied the roughness Froude number name that is now commonly used.

Although many researchers have related the roughness Froude number to the location and flow properties of the air inception point, none have explored the possibility that it could also serve as a fundamental indicator—like the flow Froude number and similar dimensionless numbers applied in other fields—of important shifts in mechanical behavior. Considering that possibility here reveals that incorporating cos(θ) into the roughness Froude number in place of sin(θ) produces a dimensionless number with relatively constant values over a broad range of slopes at the threshold between nappe and transitional skimming flow. A roughness Froude number defined in that way could serve a purpose similar to the traditional flow Froude number $F = 1$ that divides subcritical and supercritical flow. An open question that remains is whether there may be other important mechanical features of flow in relatively smooth (i.e., non-stepped) chutes that can also be explained by the roughness Froude number. One possibility may be the formation of roll waves or slug flow in open channel chutes. A recent study (Di Cristo et al. 2010) does not employ the roughness Froude number but suggests that channel roughness can have some influence.

Acknowledgements

The author greatly appreciates the contributions of the anonymous reviewers and associate editor who made insightful comments that led to significant improvement of the paper, especially the suggested alternate physical interpretation of F_* as a combination of the friction factor and relative submergence of roughness elements.

Notation

D = flow depth (m)
D_i = flow depth at aeration inception point (m)
d = stone diameter (m)
d_c = critical depth, $(q^2/g)^{1/3}$, (m)
F = Froude number (-)
F_S = stone Froude number (-)
F_W = walking Froude number (-)
F_* = roughness Froude number (-)

f = Darcy friction factor (-)g = acceleration due to gravity (m s^{-2})

h = step height measured vertically (m)

k_s = reference measure of surface roughness (m)

L = characteristic leg length or hip joint height for walking Froude number (m)

q = unit discharge (m^2 s^{-1})

S = sin θ = slope of chute (elevation change per unit distance along slope) (-)

v = velocity of walking or running (m s^{-1})

V = flow velocity (m s^{-1})

V_i = flow velocity at aeration inception point (m s^{-1})

x_i = flow distance traveled along the channel surface to the aeration inception point (m)

Z = vertical distance from spillway crest to aeration inception point (m)

β = dimensionless velocity, $F_W^{1/2}$, (-)

δ = boundary layer thickness (m)

ϵ = sand-grain roughness of flow surface, rugosity (m)

θ = slope angle of chute, measured from horizontal (-)

References

Aguirre-Pe, J., Olivero, M. L., & Moncada, A. T. (2003). Particle densimetric Froude number for estimating sediment transport. *Journal of Hydraulic Engineering*, *129(6)*, 428-437. doi:10.1061/(ASCE)0733-9429(2003)129:6(428)

Alexander, R. M. (1984). The gaits of bipedal and quadrupedal animals. *International Journal of Robotics Research, 3(2)*, 49-59. doi:10.1177/027836498400300205.

Alexander, R. M. (1989). Optimization and gaits in the locomotion of vertebrates. *Physiological Reviews, 69(4)*, 1199-1227. doi:10.1152/physrev.1989.69.4.1199

Alexander, R. M. (2005). Models and the scaling of energy costs for locomotion. *Journal of Experimental Biology, 208*, 1645-1652. doi:10.1242/jeb.01484

Alexander, R. M. & Jayes, A. S. (1983). A dynamic similarity hypothesis for the gaits of quadrupedal mammals. *Journal of Zoology, 201*, 135-152. doi:10.1111/j.1469-7998.1983.tb04266.x

Amador, A., Sánchez-Juny, M. & Dolz, J. (2009). Developing flow region and pressure fluctuations on steeply sloping stepped spillways. *Journal of Hydraulic Engineering, 135(12)*, 1092-1100. doi: 10.1061/(ASCE)HY.1943-7900.0000118

Bauer, W. J. (1954). Turbulent boundary layer on steep slopes. *Transactions of the American Society of Civil Engineers, 119*, 1212-1232, Paper No. 2719. doi: 10.1061/TACEAT.0006971

Bauer, W. J. (1966). Discussion of 'Boundary layer development and spillway energy losses'. *Journal of the Hydraulics Division, 92(HY2),* 373-378. doi: 10.1061/JYCEAJ.0001429

Biewener, A. A. (1989). Scaling body support in mammals: limb posture and muscle mechanics. *Science, 245,* 45-48. doi:10.1126/science.2740914

Boes, R. M. & Hager, W. H. (2003a). Two-phase flow characteristics of stepped spillways. *Journal of Hydraulic Engineering, 129(9)*, 661-670. doi:10.1061/(ASCE)0733-9429(2003)129:9(661)

Boes, R. M. & Hager, W. H. (2003b). Hydraulic design of stepped spillways. *Journal of Hydraulic Engineering, 129(9)*, 671-679. doi:10.1061/(ASCE)0733-9429(2003)129:9(671)

Boes, R. M. & Minor, H.-E. (2000). Guidelines for the hydraulic design of stepped spillways. In: *Hydraulics of Stepped Spillways*, Proceedings of the International Workshop on Hydraulics of Stepped Spillways, Zurich, Switzerland. Minor, H.-E. & Hager, W. H., eds. London: CRC Press.

Cain, P. (1978). Measurements within self-aerated flow on a large spillway. Ph.D. thesis, University of Canterbury, Christchurch, New Zealand. doi: 10.26021/2148

Cain, P. & Wood, I. R. (1981). Measurements of self-aerated flow on a spillway. *Journal of the Hydraulics Division, 107(HY11)*, 1425-1444. doi: 10.1061/JYCEAJ.0005761 [Erratum in *J. Hydraul. Eng.*, 1983, *109(1)*, 145-146. doi:10.1061/(ASCE)0733-9429(1983)109:1(145)]

Campbell, F. B., Cox, R. G. & Boyd, M. B. (1965). Boundary layer development and spillway energy losses. *Journal of the Hydraulics Division, 91(HY3)*, 149-163. doi: 10.1061/JYCEAJ.0001235

Cassidy, J. J. (1966). Discussion of 'Boundary layer development and spillway energy losses'. *Journal of the Hydraulics Division, 92(HY2)*, 370-372. doi: 10.1061/JYCEAJ.0001429

Chanson, H. (1994a). Hydraulics of skimming flows over stepped channels and spillways. *Journal of Hydraulic Research, 32(3)*, 445-446. doi:10.1080/00221689409498745

Chanson, H. (1994b). *Hydraulic design of stepped cascades, channels, weirs and spillways*. Pergamon.

Chanson, H. (2002). *The hydraulics of stepped chutes and spillways*. A. A. Balkema.

Chanson, H. & Toombes, L. (2004). Hydraulics of stepped chutes: The transition flow, *Journal of Hydraulic Research, 42(1)*, 43-54, doi: 10.1080/00221686.2004.9641182

Cheng, X., Gulliver, J. S. & Zhu, D. (2014). Application of displacement height and surface roughness length to determination boundary layer development length over stepped spillway. *Water, 6(12)*, 3888–3912. doi: 10.3390/w6123888

Chow, V. T. (1959). *Open-channel hydraulics*. McGraw-Hill.

Di Cristo, C., Iervolino, M, Vacca, A. & Zanuttigh, B. Influence of relative roughness and reynolds number on the roll-waves spatial evolution. *Journal of Hydraulic Engineering, 136(1),* 24-33. doi: 10.1061/(ASCE)HY.1943-7900.0000139

Ettema, R., Arndt, R., Roberts, P. & Wahl, T. (2000). *Hydraulic modeling concepts and practice.* American Society of Civil Engineers Manual No. 97. doi: 10.1061/9780784404157

Felder, S. & Chanson, H. (2009). Energy dissipation, flow resistance and gas-liquid interfacial area in skimming flows on moderate-slope stepped spillways. *Environmental Fluid Mechanics, 9*, 427–441. doi: 10.1007/s10652-009-9130-y

Felder, S. & Chanson, H. (2011). Energy dissipation down a stepped spillway with nonuniform step heights. *Journal of Hydraulic Engineering, 137(11)*, 1543-1548. doi: 10.1061/(ASCE)HY.1943-7900.0000455

Felder, S. & Chanson, H. (2013). Aeration, flow instabilities, and residual energy on pooled stepped spillways of embankment dams. *Journal of Irrigation and Drainage Engineering, 139(10),* 880-887. doi: 10.1061/(ASCE)IR.1943-4774.0000627

Felder, S. & Chanson, H. (2016). Simple design criterion for residual energy on embankment dam stepped spillways. *Journal of Hydraulic Engineering*, *142(4)*, 04015062. doi: 10.1061/(ASCE)HY.1943-7900.0001107

Frizell, K. W. & Frizell, K. H. (2015). *Guidelines for hydraulic design of stepped spillways*. Hydraulic Laboratory Report HL-2015-06. U.S. Dept. of the Interior, Bureau of Reclamation, Denver, Colorado.

Gangadharaiah, T., Lakshmana Rao, N. S. & Seetharamiah, K. (1970). Inception and entrainment in self-aerated flows. *Journal of the Hydraulics Division, 96(HY7)*, 1549-1565. doi: 10.1061/JYCEAJ.0002566

Gibb, A., Jayne, B. & Lauder, G. (1994). Kinematics of pectoral fin locomotion in the bluegill sunfish *lepomis macrochirus*. *Journal of Experimental Biology, 189,* 133-161. doi: 10.1242/jeb.189.1.133

Hager, W. H & Boes, R. M. (2000). Backwater and drawdown curves in stepped spillway flow. In: *Hydraulics of Stepped Spillways*, Proceedings of the International Workshop on Hydraulics of Stepped Spillways, Zurich, Switzerland. Minor, H.-E. & Hager, W. H., eds. London: CRC Press.

Halbronn, G. (1952). Étude de la Mise en Régime des Écoulements Sur les Ouvrages à Forte Pente, *La Houille Blanche*, *38:(1)*, 21-40, doi:10.1051/lhb/1952018

Halbronn, G. (1954). Discussion of 'Turbulent boundary layer on steep slopes'. *Transactions of the American Society of Civil Engineers, 119*, 1234-1240. doi: 10.1061/TACEAT.0007019

Hale, M. E., Day, R. D., Thorsen, D. H. & Westneat, M. W. (2006). Pectoral fin coordination and gait transitions in steadily swimming juvenile reef fishes. *Journal of Experimental Biology, 209*, 3708-3718. doi:10.1242/jeb.02449

Hiller, P. H., Lia, L. & Aberle, J. (2019). Field and model tests of riprap on steep slopes exposed to overtopping, *Journal of Applied Water Engineering and Research, 7(2)*, 103-117. doi:10.1080/23249676.2018.1449675

Hohermuth, B., Boes, R. M. & Felder, S. (2021) High-velocity air–water flow measurements in a prototype tunnel chute: scaling of void fraction and interfacial velocity. *Journal of Hydraulic Engineering, 147(11)*, 04021044. doi: 10.1061/(ASCE)HY.1943-7900.0001936

Hunt, S. L. & Kadavy, K. C. (2013). Inception point for embankment dam stepped spillways. *Journal of Hydraulic Engineering, 139(1),* 60-64. doi:10.1061/(ASCE)HY.1943-7900.0000644

Hunt, S. L., Kadavy, K. C. & Hanson, G. J. (2014). Simplistic design methods for moderate-sloped stepped chutes. *Journal of Hydraulic Engineering, 140(12)*. doi:10.1061/(ASCE)HY.1943-7900.0000938

Hunt, S.L., Kadavy, K. C., Wahl, T. L. & Moses, D. W. (2022). Physical modeling of beveled-face stepped chute. *Water, 14(3)*, 365. doi:10.3390/w14030365

Keller, R. J. (1972). Field measurement of self-aerated high speed open channel flow. Ph.D. thesis, University of Canterbury, Christchurch, New Zealand. doi: 10.26021/1896

Keller, R. J., Lai, K. K. & Wood, I. R. (1974). Developing region in self-aerated flows. *Journal of the Hydraulics Division, 100(HY4)*, 553-568. doi: 10.1061/JYCEAJ.0003932

Keller, R. J. & Rastogi, A. K. (1975). Prediction of flow development on spillways. *Journal of the Hydraulics Division, 101(HY9)*, 1171-1184. doi: 10.1061/JYCEAJ.0004414

Keller, R. J. & Rastogi, A. K. (1977). Design chart for predicting critical point on spillways. *Journal of the Hydraulics Division, 103(HY12)*, 1417-1429. doi: 10.1061/JYCEAJ.0004889

Killen, J. M. (1968). The surface characteristics of self aerated flow in steep channels. Ph.D. thesis, Univ. Minnesota, Minneapolis, MN.

Kramer, M., & Chanson, H. (2018). Transition flow regime on stepped spillways: air–water flow characteristics and step-cavity fluctuations. *Environmental Fluid Mechanics, 18(4)*, 947-965. doi: 10.1007/s10652-018-9575-y

Lai, K. K. (1971). Studies of air entrainment in steep open channels, M. Eng. thesis, University of New South Wales, Sydney, Australia.

Lane, E. W. (1939). Entrainment of air in swiftly flowing water. *Civil Engineering, 9(2)*, 89–91. ASCE.

Levi, E. (1967). Macroturbulence produced by vortex breakdown in high velocity flows. *Proceedings of the 12th Congress of IAHR*, Vol. 2, 1967, pp. 54-60.

Mateos, C. & Elviro, V. (1997). Initiation of aeration in stepped spillways. In: *Energy and Water: Sustainable Development, Proceedings of the 27th Congress of IAHR*.

Meireles, I. & Matos, J. (2009). Skimming flow in the nonaerated region of stepped spillways over embankment dams. *Journal of Hydraulic Engineering, 135(8)*, 685-689. doi:10.1061/(ASCE)HY.1943-7900.0000047

Monin, A. M. & Yaglom, A. S. (1971). *Statistical Fluid Mechanics – Vol. 1: Mechanics of Turbulence* (J. L. Lumley, Ed.), MIT Press.

Ohtsu, I., Yasuda, Y. & Takahashi, M. (2001). Discussion of onset of skimming flow on stepped spillways. *Journal of Hydraulic Engineering, 127(6)*, 519–525. doi: 10.1061/(ASCE)0733-9429(2001)127:6(519)

Ohtsu, I., Yasuda, Y. & Takahashi, M. (2004). Flow characteristics of skimming flows in stepped channels. *Journal of Hydraulic Engineering, 130(9)*, 860–869. doi:10.1061/(ASCE)0733-9429(2004)130:9(860)

Pfister, M. & Chanson, H. (2014). Two-phase air-water flows: Scale effects in physical modeling. *Journal of Hydrodynamics, 26(2)*, 291-298. doi:10.1016/S1001-6058(14)60032-9

Rayner, J., Jones, G. & Thomas, A. (1986). Vortex flow visualizations reveal change in upstroke function with flight speed in bats. *Nature, 321*, 162-164. doi:10.1038/321162a0

Straub, L. & Anderson, A. (1958). Experiments on self aerated flow in open channels. *Journal of the Hydraulics Division, 84(HY7)*, 1-35. doi: 10.1061/JYCEAJ.0000261

Terrier, S. (2016). Hydraulic performance of stepped spillway aerators and related downstream flow features. Thesis No. 6989, École Polytechnique Fédérale de Lausanne (EPFL). https://infoscience.epfl.ch/record/218528?ln=fr

Valero, D. & Bung, D. B. (2016). Development of the interfacial air layer in the non-aerated region of high-velocity spillway flows. Instabilities growth, entrapped air and influence on the self-aeration onset. *International Journal of Multiphase Flow*, 84, 66-74. doi:10.1016/j.ijmultiphaseflow.2016.04.012

Vaughan, C. L. & O'Malley, M. J. (2005). Froude and the contribution of naval architecture to our understanding of bipedal locomotion. *Gait and Posture*, 21(3), 350-362. doi:10.1016/j.gaitpost.2004.01.011

Wood, I. R., Ackers, P. & Loveless, J. (1983). General method for critical point on spillways. *Journal of Hydraulic Engineering*, 109(2), 308-312. doi:10.1061/(ASCE)0733-9429(1983)109:2(308)

List of figures

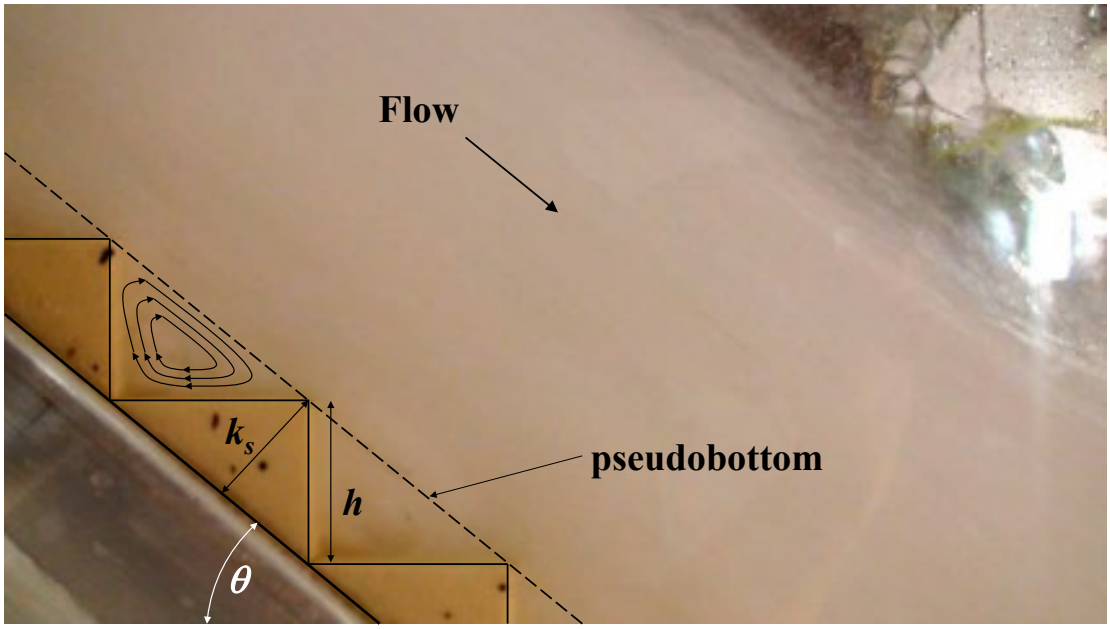

Figure 1 Skimming flow in a stepped chute on a 0.8:1 (h:v) slope (51.3°). Adapted from Frizell & (Frizell 2015).

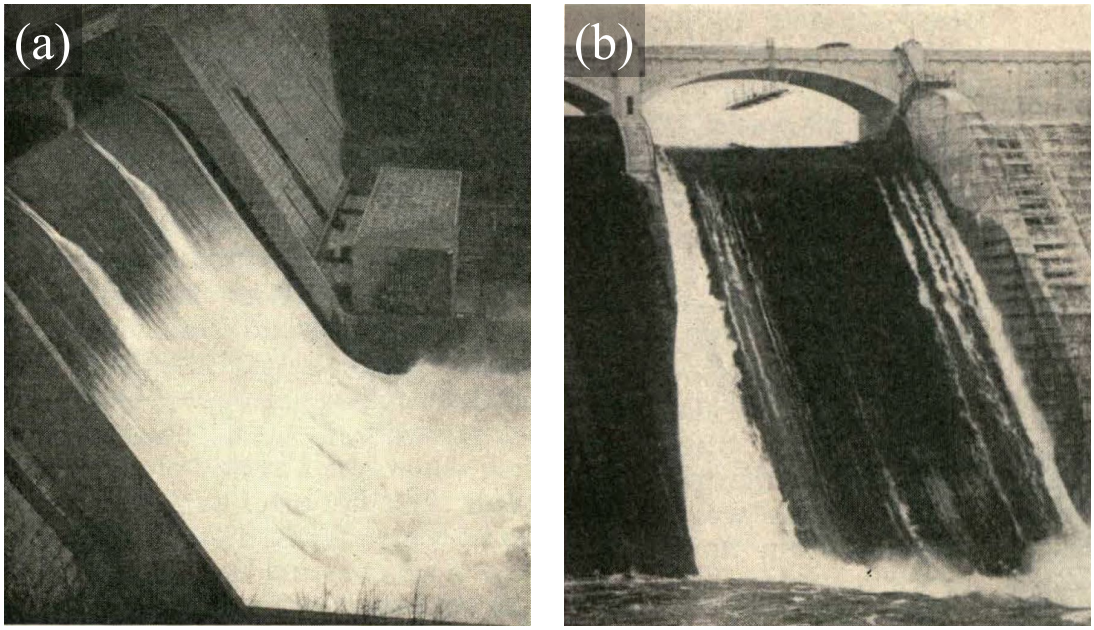

Figure 2 Photos show: (a) inception of aerated flow midway down the face of 81-m (265-ft) high Norris Dam (Tennessee) at $Q = 368$ m^3 s^{-1} (13,000 ft^3 s^{-1}), $q = 4.0$ m^2 s^{-1} (43 ft^2 s^{-1}); (b) non-aerated flow (except along edges) through one gate of 67-m (220-ft) high Madden Dam (Panama) at $Q = 456$ m^3 s^{-1} (16,100 ft^3 s^{-1}), $q = 15.0$ m^2 s^{-1} (161 ft^2 s^{-1}). Adapted from Lane (1939). Every effort has been made to trace the copyright holders and obtain permission to reproduce this image. Please contact the publisher with any enquiries or any information relating to this image or the rights holder.

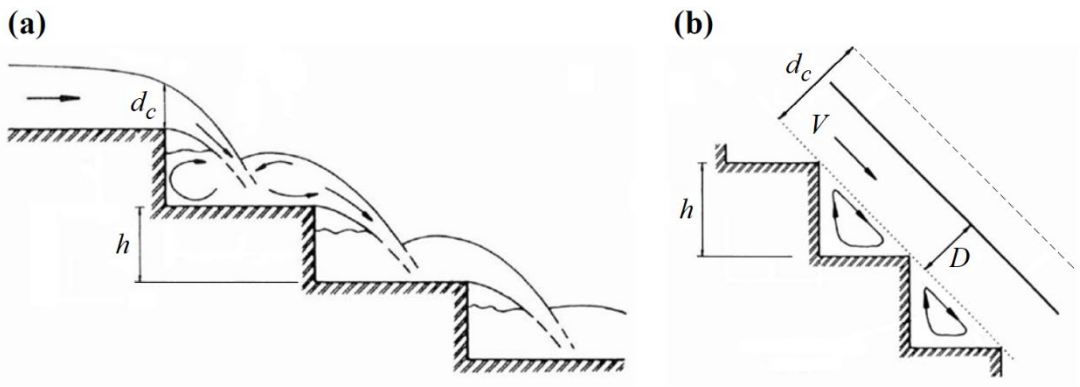

Figure 3 Flow mechanics of (a) nappe and (b) skimming flows in stepped chutes. Adapted from Chanson (1994a).

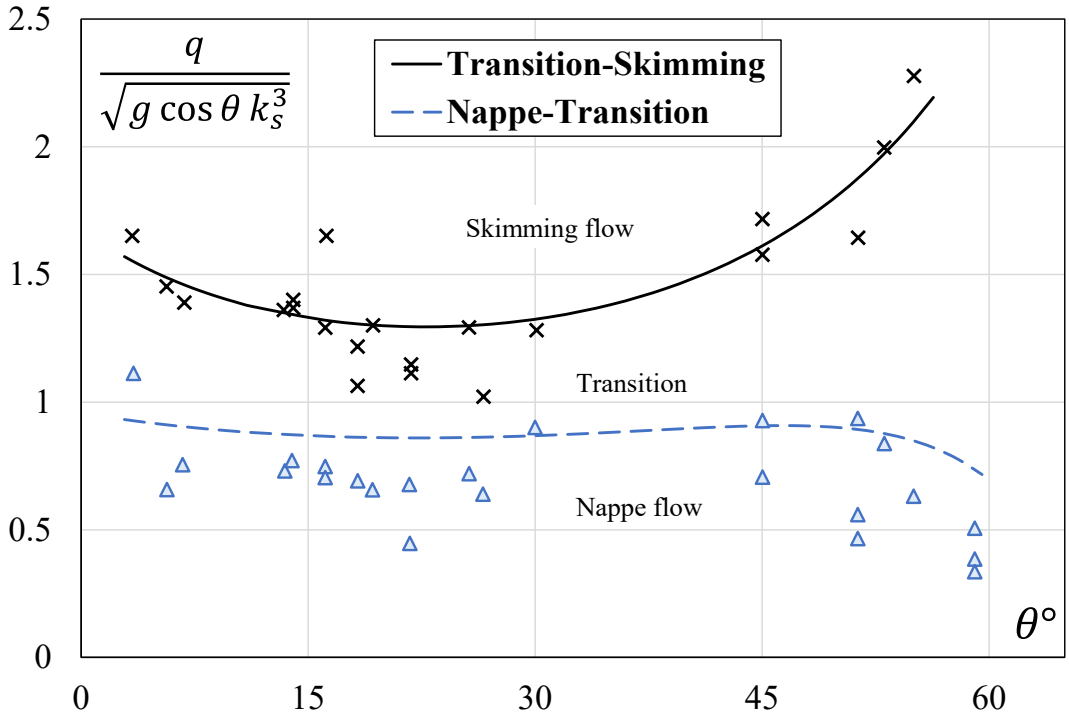

Figure 4 Values of $q/(g \cos \theta \, k_s^3)^{1/2}$ and curves fit to data at thresholds between nappe, transitional, and skimming flows. Curves developed and data compiled by Kramer & Chanson (2018).

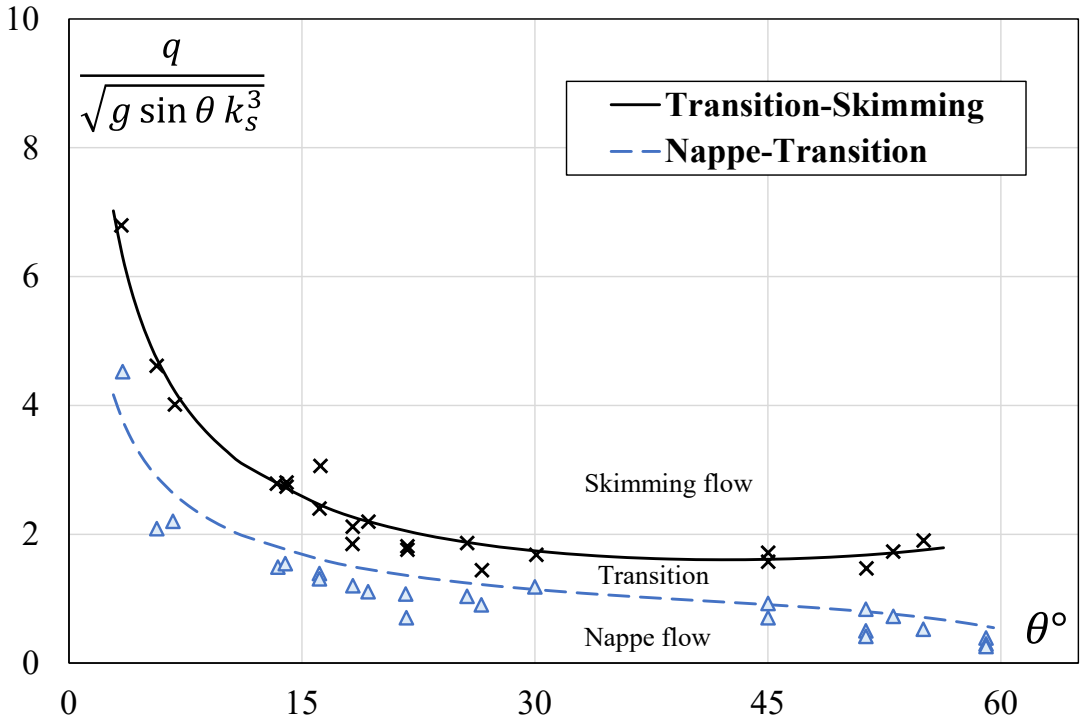

Figure 5 Values of $q/(g \sin \theta \, k_s^3)^{1/2}$ and curves fit to data at thresholds between nappe, transitional, and skimming flows. Curves developed and data compiled by Kramer & Chanson (2018).